PAPER • OPEN ACCESS

Optimization of Francis Turbine Runner for Variable Speed Operations with minimization of sediment erosion

To cite this article: Amul Ghimire *et al* 2022 *IOP Conf. Ser.: Earth Environ. Sci.* **1079** 012029

Optimization of Francis Turbine Runner for Variable Speed Operations with minimization of sediment erosion

Amul Ghimire[1], Saroj Gautam[1], Sailesh Chitrakar[2*] and Hari Prasad Neopane[2]

[1] Turbine Testing Lab, Kathmandu University, P.O. Box 6520, Dhulikhel, Nepal
[2]Department of Mechanical Engineering, Kathmandu University, P.O. Box 6520, Dhulikhel, Nepal

E-mail: sailesh@ku.edu.np

Abstract. Sediment erosion is one of the most notorious phenomenon damaging the turbines, in the Himalayan region. Francis turbine, which is one of the most used type of hydro turbine in the world as well as in Nepal, is affected quite severely, more so when operated in off design conditions. This study has taken a reference design of a Francis turbine from a hydropower in Nepal to optimize it for operation in variable speeds. Minimization of sediment erosion and maximization of efficiency are taken as the objective functions of the optimization, for which blade angles at trailing edge and blade angle distribution are taken as the design variables. The design space of the runner are constrained such that the optimized design could replace the existing runner in the turbine. Latin Hypercube Sampling technique is used to populate the design space such that the design variables are divided randomly to create required number of designs in the design space. Computational Fluid Dynamic analysis are performed on simplified numerical models of the samples to predict their performance and Sediment Erosion Rate Density (SERD), under various operating conditions. The results of output parameters, obtained from CFD, along with the design variables, are used to develop an approximation model relating the objective functions with the design parameters. NSGA-II optimization technique is used to search for the optimum design. The paper presents the comparison of the sediment erosion and efficiency of the reference runner and optimized runners under various operating conditions. It also presents an outline of the process used to optimize the runner for variable speed operation with minimum sediment erosion.

1. Introduction

The design of hydraulic turbines are usually based on achieving maximum efficiency and cavitation performance, among others[1]. The design procedure is optimal considering that the waters in the European and North American rivers contain very less amount of sediment, posing almost no threat to the turbine in terms of sediment erosion[2]. However, for hydropower projects located in the Himalayan region, damages caused due to sediment erosion is one of the most important factor forcing the maintenance within just one year in contrast to decades long maintenance period in the European hydropower projects[3]. The mountains in this region are geologically fragile, with young and rising mountains[4]. The fragile rocks breakdown easily due to natural phenomenon, such as monsoon precipitations, earthquake, landslides, wind, etc. The sediment particles thus formed are transported downstream with the river water[5]. The most common method used by the turbine manufacturers to tackle the erosion caused by sediment particles is to apply coating on blade surface[6][7]. In addition to that, several researchers have attempted to modify the hydraulic profile of the runner blade to reduce the effect of sediment particle on the blade surface[8][1][9].

More than 60% of the total power produced by the hydropower around the world are produced using Francis turbines[10]. The case is similar for Nepal with around 75% of the hydropower being compatible for installation of Francis turbines[11]. Even though the turbine is highly efficient, it is not safe from damages caused by the sediment in the water. Moreover, it has been found that the Francis turbines require repair and maintenance more frequently, due to severe sediment erosion implicated on the turbine[12]. According to several power plant operators interacted by the authors of this article, hydropower plants are operated in part load and full load conditions quite often. Gautam et. al[13] have concluded that Francis turbines are more severely eroded when operated in off design conditions. This happens because these turbines are not designed to be operated in sediment laden water and even more so to be operated in off design conditions with high concentration of sediment in the water.

Variable speed Francis turbines are being developed in Europe to meet their requirement of flexibility in the grid brought about by intermittent sources of renewable power like wind and solar[14]. Variable speed operation of Francis turbines are associated with reduction in fatigue and wear and higher efficiency at off design conditions[15]. Applications of variable speed Francis turbines in hydropower prone to sediment erosion can be pivotal, considering the findings of the previous research. This research work has thus been initiated to develop a Francis turbine with variable speed capability and minimum sediment erosion. One of the sediment affected hydropower plant has been chosen as a reference case for this research. The specific details of the project cannot be disclosed at this time due to the non-disclosure agreement. This paper describes the procedure used for optimization of the Francis turbine runner that will replace the existing runner in the site.

Currently, there are two methods to facilitate the turbine to change its speed continuously. The first method is by using a fully fed frequency converter, also known as Full Size Frequency Converter (FSFC). In this method, the FSFC is used between the synchronous generator and the grid[16]. The state of the art in the technology has allowed a loss of 1.5% to 2% for hydropower up to 100 MW[17]. The technology is already in action in a pump storage project of 160 MW. The second method is the use of an asynchronous generator, also known as Doubly Fed Induction Machine. The speed of the machine can be varied in a range of ±10% of the synchronous speed allowing a power variation of ±30%[18].

2. Methodologies

The strategy used to optimise the design of Francis turbine for variable speed operation is shown in Figure 2 The baseline turbine design, Numerical Modelling, DOE & RSM modelling and Multi Objective Genetic Algorithm are the major steps used in the optimization process.

2.1.Turbine Design

The cost of upgrading a conventional hydropower operating at synchronous speed to a variable speed is so high that, it is not economically viable justifiable at this time[15]. In addition to that, the efficiency of the frequency converter, which is generally in the range of 92-95% thus using this technology could undermine the efficiency improvement that might come after the optimization of the turbine, especially at the BEP. Thus, it is important to bypass the frequency converter when the turbine is being operated at BEP, where the efficiency is already so high that there is not much room for improvement. However, its importance during off design operations could be justifiable as the efficiency drop is still very high under such operating conditions. Thus, the base design of variable speed Francis turbine follows the same process as a synchronous speed turbine.

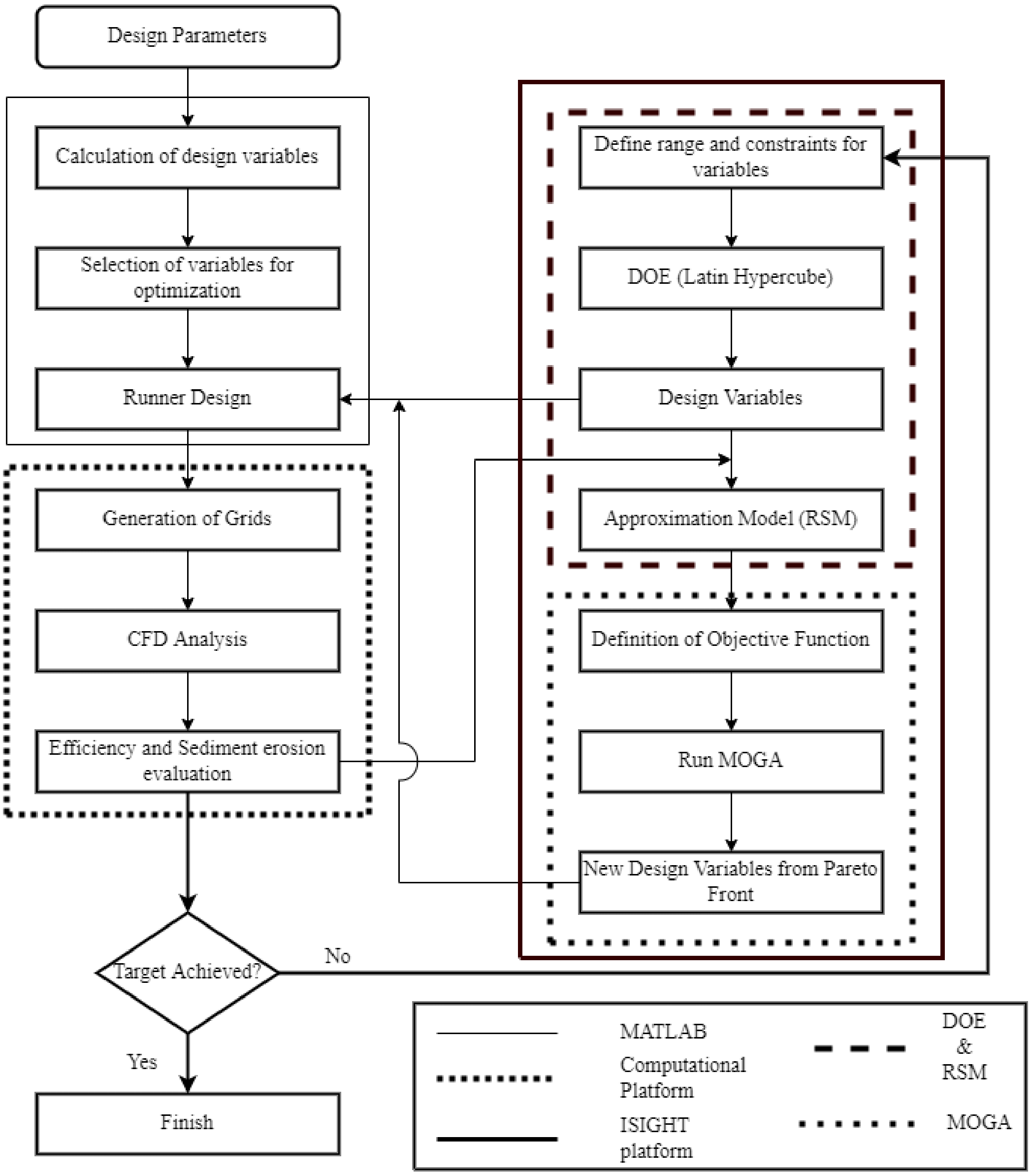

Figure 1. Multi Objective Optimization Flow Diagram

In this case, the base design of the runner has been developed using Bovet method, in a MATLAB based application, which was developed by the author of this paper, at Turbine Testing Laboratory. As the major objective of this study is to replace the pre-existing runner at the reference site, the size of the runner itself could not be hindered. Thus, few modifications were made in the software to incorporate the constraints introduced due to size of the pre-existing runner. The diameter at the inlet of the runner was unchanged, so that the clearance gap between the guide vane facing plates and the labyrinth seal, which in this case was engraved at the inlet, on shroud/band as well as hub of the runner. Similarly, the inlet height of the runner was also kept constant, as the height of the guide vane could not be changed during this study. In addition to that, the diameter at the outlet of the runner, i.e shroud diameter was also unchanged because the diameter of the draft tube cone connected to it was fixed. Either increasing or decreasing the diameter of the outlet could affect the flow condition at the transition between the runner and draft tube. No changes were made in the overall height of the runner as well. The dimensions that were kept constant in the runner have been portrayed in the Figure below.

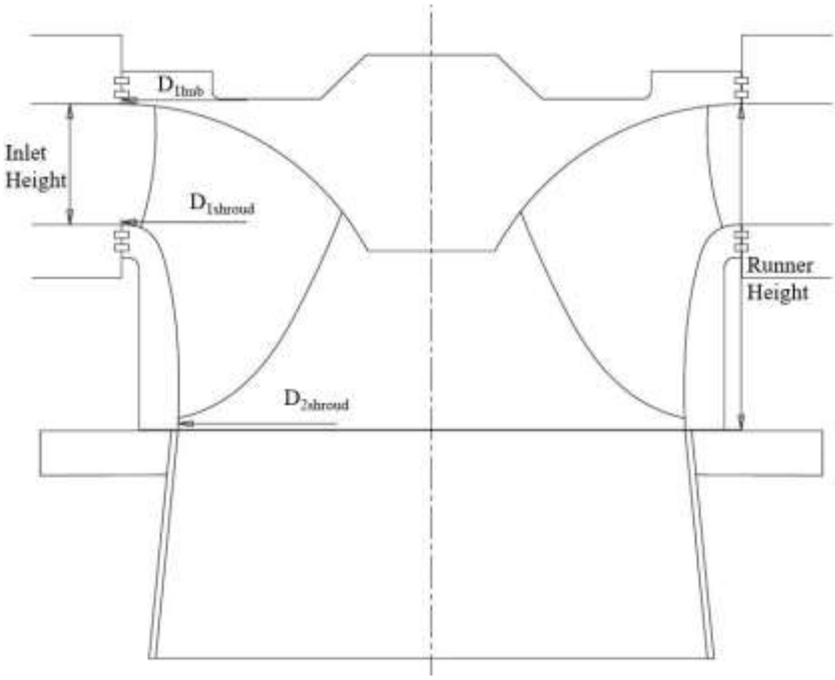

Figure 2. Fixed major dimensions of the runner in meridional plane

The characteristic curves defining the hub and shroud depend on a non-dimensional specific speed (υ_Λ), calculated using equation 1. Generally, a discharge coefficient is selected based on this specific speed value, which is then used to calculate the radius at which the shroud intersect with the trailing edge. However, the diameter at the outlet of the runner was fixed, based on which the value of the discharge coefficient was calculated and it was found that the flow coefficient determined in such a way was slightly greater than the one determined based on the value of υ_Λ. It is common practice to change the value of discharge coefficient during the design process based on designer's experiences and instincts.

$$\nu_\Lambda = \frac{\omega(Q_\Lambda/\pi)^{1/2}}{(2.E_\Lambda)^{3/4}} \tag{1}$$

Where,

ω = Angular speed of the runner
E_Λ = Specific hydraulic energy
Q_Λ = Discharge at BEP

$$R_{2e} = \sqrt[3]{\frac{Q/\pi\omega}{\varphi_{2e}}} \tag{2}$$

Where,

R_{2e} = Radius at outlet of runner (intersection of shroud and trailing edge)
φ_{2e} = Discharge Coefficient

The diameter of hub and shroud at the inlet of the runner were also used from the existing runner, instead of calculating them separately, as it is usually done. All other quantities required to develop the curves were calculated based on the non-dimensional specific speed. The leading and trailing edge are developed considering them a parabolic curves with their vertex on shroud, having the axis parallel to the axis of runner and passing through a specific point on the hub. After defining the required number of streamlines between the hub and shroud, meridional view of the runner is finalized. The radial view of the runner is developed by using a method called 'Conformal Mapping'. An imaginary plane called

GH plane is defined, which is used to transform the each point on the streamlines, in meridional plane, into radial plane. 'G' is the length of streamline in the meridional plane while 'H' is the length of the streamline in radial plane. In order to find the relation between 'G' and 'H', the blade angle (β) at each point on the streamline is required. In order to find the β at each point on the streamline, β at the first and last point on the streamline, cropped within the blade portion, is required. The β at leading and trailing edge can be determined using the equation (3) and equation (4) respectively[19]. After determining the values of β at the two extremes, blade angle can be distributed along the length of the streamline in any way, the designer wants. One of the most common way of distributing the value of β along the length of streamline is by dividing the β linearly between the β calculated at leading edge and trailing edge, which was adopted for the baseline design as well.

$$\cot \beta_1 = \frac{\pi D_1 B_1}{Q}\left(\frac{\pi D_1^* N}{60} - \frac{60 g H}{\pi D_1^* N}\right) \tag{3}$$

Where,

D_1 = Diameter at the intersection of leading edge and shroud
D_1^* = Diameter at the point, where β is being evaluated
N = Rotational speed in rpm

$$\tan \beta_2 = \frac{60 \cdot Q}{\pi D_2^* N A_2} \tag{4}$$

Where,

D_2^* = Diameter at the point, where β is being evaluated
A_2 = Area at the outlet of the runner

$$\tan \beta = \frac{\Delta G}{\Delta H} \tag{5}$$

Where,

ΔG = Length of a section of streamline in meridional plane
ΔH = Length of the section of streamline in radial plane

$$d\theta = \frac{\Delta H}{R} \tag{6}$$

Where,

$d\theta$ = Change in theta in radial plane
R = Radius at the point of interest on streamline

The radial view of the blade can be determined by evaluating the value of theta at each point on the streamlines. Z and R components are determined in the meridional view while θ and R components are determined in the radial view. Thus, 3D blade profile of the blade camber can be determined after combining all three components in a cylindrical coordinate system. Adding the thickness to the camber surface creates a blade with thickness. Modified Eppler 472 airfoil was used to provide the thickness profile to the blade.

2.2.Numerical Modelling

The baseline design obtained from the MATLAB, which is extracted as a single passage domain of the runner; is discretized in ANSYS TurboGrid; to obtain high quality hexahedral mesh. 1,000,000 elements were generated in a single passage domain of the runner. The average value of y+ in the near wall regions of the rotating domain was less than 30. Reynolds Averaged Navier-Stokes (RANS) equations were solved for an incompressible flow defined in the model discussed earlier. Total pressure in stationary frame, boundary condition was defined at the inlet of the fluid passage, with the direction of the flow defined using cylindrical flow components. The angle of incidence was varied from 14^o to 23^o in a step of 1^o radially while the axial component was set to 0 for all the opening angles. The maximum guide vane opening was restrained up to 23º in the reference turbine, which is why no numerical simulations were performed beyond 23º guide vane opening. Static pressure boundary condition with relative pressure of 0 pascal was set at the outlet of the passage which was extended far from the outlet of the runner. The rpm was varied from 650 rpm to 850 rpm, with 50 rpm steps, at each guide vane opening. The numerical simulations were performed in steady-state, with Shear Stress Transport (SST) turbulence model.

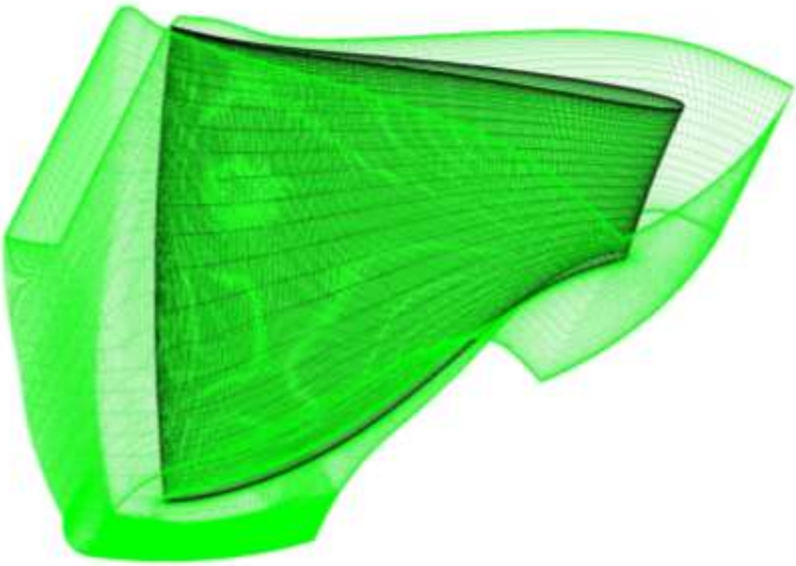

Figure 3. Numerical model of a single blade passage of runner with hexahedral mesh

2.3.Erosion Model

As the major objective of the study was to reduce the erosion on the runner, predicting the sediment erosion on the blade surface correctly is the most important task in the study. In order to make use of the erosion models in the ANSYS CFX, Eularian-Lagrangian scheme is to be used. The water and sediment are defined separately as continuous fluid and particle transport solid. The density, size, shape and concentration of the particles are defined based on the sediment analysis report of the reference site during flood. Considering that the major part of the sediment in the river is covered by quartz, which is also the ingredient in the sediment which causes damage to the turbine surface, its properties are provided to the sediment particle in the CFX. Tabakoff & Grant and Finnie erosion model are available in ANSYS CFX which have been used by several researchers to predict the sediment erosion on hydraulic machines. Finnie erosion model solves different angles of attack on surface separately, thus predicting the sediment erosion rate density based on particle impact velocity[20]. While, Tabakoff & Grant erosion model combines all the angles of attack of the sediment particles to compute the sediment erosion. It also considers other parameters like velocity, material properties, etc thus predicting the sediment erosion rate more accurately[13]. Several researchers prefer this erosion model to predict the sediment erosion rate in hydraulic turbines, more specifically in Francis turbine[21][22]. The underlying equations used by Tabakoff & Grant erosion model has been given in equations below[23]:

$$E = f(\gamma)\left(\frac{V_p}{V_1}\right)^2 cos^2\gamma\,(1 - R_T^2) + f(V_{PN}) \tag{7}$$

Where,

$$f(\gamma) = \left[1 + k_2 k_{12}\, sin\left(\gamma\frac{\pi/2}{\gamma_0}\right)\right]^2 \tag{8}$$

$$R_T = 1 - \frac{V_P}{V_2} sin\,\gamma \tag{9}$$

$$f(V_{PN}) = \left(\frac{V_P}{V_N} sin\, \gamma\right)^4 \quad (10)$$

$$k_2 = \begin{cases} 1.0 & if\ \gamma \leq 2\gamma_0 \\ 0.0 & if\ \gamma > 2\gamma_0 \end{cases} \quad (11)$$

E is dimensionless mass (mass of eroded wall material per unit mass of the particle)
V_p is the particle impact velocity
γ is the impact angle in radians
γ_0 is the angle of maximum erosion
k_1 *to* k_4, k_{12} *and* γ_0 are constants depending on particle and wall materials.

Table 1. Tabakoff Constants in CFX-Pre[23]

Value	Dimensions	CFX-Pre Variables
k_{12}	(dimensionless)	K12 constant
k_2	(dimensionless)	
V_1	[ft/s]	Reference velocity 1
V_2	[ft/s]	Reference velocity 2
V_3	[ft/s]	Reference velocity 3
γ_0	[deg]	Angle of maximum erosion

The overall erosion rate is given by:

$$Erosion\ Rate = E * N * m_p \quad (12)$$

Where,
M_p is the mass of the particle
N is the number rate of the particles

The Tabakoff constant values for Quartz-Steel was used during this study. The massflow rate of the sediment was calculated considering 6000ppm of sediment in the water. Sediment erosion rate density was calculated at all the conditions mentioned in the previous section. Average of sediment erosion rate density at all the operating conditions were taken to use as a variable for the optimization process.

2.4.Design of Experiment

Latin Hypercube Sampling (LHS) technique was used to generate the design matrix required to obtain an accurate approximate model. LHS is useful technique to populate the design space almost randomly for any number of designs required, as long as it is greater than the number of variables[24]. Blade angle distribution and blade angle at the trailing edge of the blade play an important role in the performance of the runner and its sediment erosion resistant characteristics. The meridional passage is discretized using 3 streamlines in its span, to reduce the computational requirement. The blade angle at the trailing edge for each streamlines are calculated as described in section 2.1, while the blade angle distribution is parametrized using a control point, in between the leading and trailing edge blade angles, which defines a quadratic Bezier curve. Thus, 3 values of β_2 and 3 values of the control points were selected as input variables, while average efficiency and average sediment erosion rate density were selected as output variables. 28 design points were developed, within the specified range of each input variables, using the LHS technique. The design points were used to generate different designs based on the variable values provided by DOE. 50 numerical simulations were carried out on each design sample to obtain the efficiency and sediment erosion rate density under various operating condition, thus carrying out 1,400 numerical simulations for 28 different designs. At different guide vane openings, results obtained for variable rotational speed are compared and the one with greater efficiency and lesser sediment erosion rate density is selected. Averages of the selected efficiency was used directly as an output parameter,

IOP Conf. Series: Earth and Environmental Science 1079 (2022) 012029 doi:10.1088/1755-1315/1079/1/012029

while the average erosion rate density was normalized by the maximum value of the complete design matrix, before using as an output parameter.

2.5.Approximation model

Response Surface Model approximation technique was used to create an approximation model for the optimization process. The variables β_{21}, β_{22}, β_{23}, C_1, C_2 and C_3 are used as the input parameters, while average efficiency and average erosion rate density are used as the output parameters. Quadratic order approximation was selected to reduce the number of design point required and to create an approximation model with satisfactory acceptance level of accuracy. Cross validation error analysis method was selected to reduce the errors in the approximation model. The baseline design was used for the cross validation error analysis. 14 coefficients for each output parameters are determined by to create an approximation equation.

2.6.Optimization

The design variables, along with the range, used in the approximation model were used in the optimization process as well. As the objectives of the study is to maximize the average efficiency and minimize the average sediment erosion, a multi-objective genetic algorithm was used to carry out the optimization. The modified Non-dominated Sorting Genetic Algorithm (NSGA-II) was used to develop a Pareto front by selecting feasible non-dominated designs. The objective functions are constrained within a realistic range to reduce approximations that are physically impossible. The ranges of all the variables used in the optimization are given in the table below.

Table 2. Design Variables and Objective Functions

	Parameters	**Types**	**Range**	**Baseline**
Input Parameters	β_{21}	Continuous	12-16	14.7
	β_{22}	Continuous	20-25	23.7
	β_{23}	Continuous	27-32	29.7
	C_1	Continuous	16-48	32.2
	C_2	Continuous	25-53	39.1
	C_3	Continuous	32-60	45.7
Output Parameters	Average η	Maximize		0.936
	Average SERD (normalized)	Minimize		0.08 ($7.2e^{-7}$)

In order to proceed the optimization, some parameters that govern the optimization process are defined. These parameters have a significant role in the results obtained from the optimization. Population size, Number of generations, Crossover probability, Crossover distribution index, and mutation distribution index and initialization mode are selected based on the sensitivity study of the parameters. 160,000 different designs of the runner were generated by the end of the optimization.

Table 3. Optimization settings

Parameters	Value
Population size	400
Number of generations	400
Crossover probability	0.9
Crossover distribution index	10
Mutation distribution index	20
Initialization mode	Random

3. Results and Discussions

The approximation model developed earlier was used to evaluate the objective functions for each design points in all the population of each generations. Based on the approximated results, a Pareto front is plotted between the two objective functions. 2 design points (D1 and D2) on the Pareto front were selected for further research. Numerical models for the runners of the selected design points were developed and numerical solutions were evaluated. The average efficiency and average sediment erosion rate density were predicted numerically, as described in section 2, to compare the results with the baseline design.

The runners modelled based on the design variables in the design points selected were different in shape and the length of the blades, in terms of appearance. The wrap angle of the initial design was 57^o at the shroud, while that of optimized designs D1 and D2 were 47^o and 45^o at shroud respectively. Similarly, the wrap angle at the hub were 56^o, 60^o and 45^o for baseline design, D1 and D2 respectively. The wrap angle dictates the length of the blade in the radial plane.

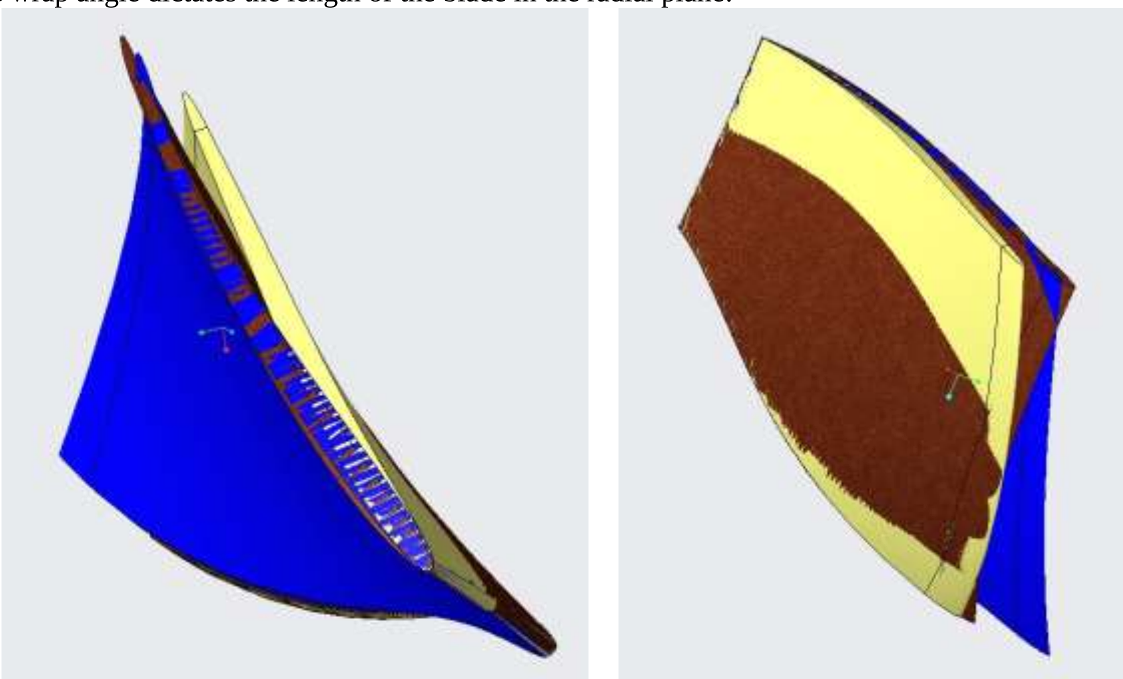

Figure 4. Comparison of Baseline design blade with designs D1 and D2

The performance of both the designs selected from the Pareto front showed an improvement in average efficiency. The efficiency at the BEP increased by 1.01% in design point D1, while it increased by 0.68% in design point D2. The average efficiency increased by 1.52% in design point D1 and by 1.14% in design point D2. Even though the performance of the blades improved, a region of low pressure, detected at the leading edge; near the shroud; increased in both the design points, as compared to the baseline design. The low pressure region could be removed by providing lean angle at the inlet of the runner, however it was not defined as one of the variables for the current case.

The second objective function of the study was average sediment erosion rate density. The average sediment erosion rate density on the baseline design blade surface was 7.2e^{-7} while the average SERD decreased to 4.7e^{-7} and 5.6e^{-7} in design points D1 and D2 respectively. Sediment erosion on all three designs were seen on towards the trailing edge, close to the shroud. Some area close to the shroud at around the 70%-80% of the blade length, were also prone to the sediment erosion. Even though the high sediment erosion prone area close to the trailing edge decreased in both design points D1 and D2, it increased at the other point. However, the average erosion rate density calculated at different operating conditions decreased in both the cases.

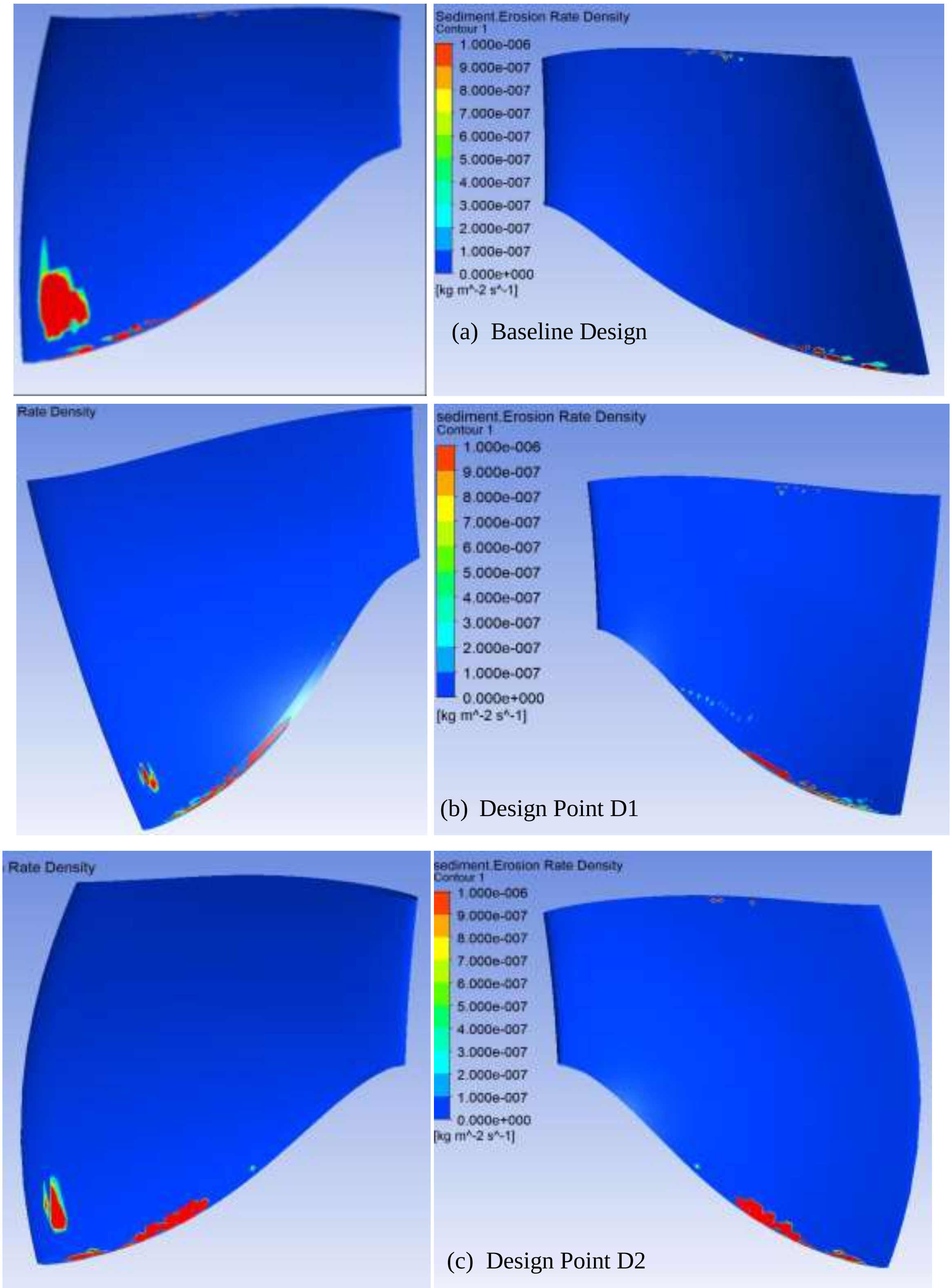

Figure 5. Sediment erosion of design points D1 and D2 compared to baseline design.

4. Conclusion

A multiobjective design optimization technique was used to design a variable speed Francis turbine for minimization of sediment erosion. A reference site was selected, for which the runner was designed such that the optimized runner would fit into the pre-existing turbine. Blade angles at trailing edge and its distribution were selected as the design variables to maximize the average efficiency and minimize the sediment erosion. A multiobjective genetic algorithm, NSGA-II optimization technique, was used to optimize the design of the runner based on the RSM approximation model developed using design points obtained from Latin Hypercube Sampling in the design space. While, the average efficiency increased by 1.52% and 1.14% in D1 and D2 respectively, the average sediment erosion rate density decreased by 34.7% and 22.22% respectively. Thus, design point D1 is selected as the optimal design of the runner.

Acknowledgments

This study was a part of MS by Research Degree at Kathmandu University. The degree is funded by EnergizeNepal project at Turbine Testing Laboratory, Kathmandu University. The study has also been supported by FranSed project. Authors would like to all the members of Turbine Testing Laboratory for their continuous support during this study. The authors would also like to thank the 'Undisclosed party' for the reference case.

References

[1] Thapa B S, Thapa B, Eltvik M, Gjosater K and Dahlhaug O G 2012 Optimizing runner blade profile of Francis turbine to minimize sediment erosion *IOP Conf. Ser. Earth Environ. Sci.* **15**
[2] Thapa B 2004 *Sand erosion in hydraulic machinery* (Norwegian University of Science and Technologt)
[3] Thapa B, Shrestha R, Dhakal P and Thapa B S 2005 Problems of Nepalese hydropower projects due to suspended sediments *Aquat. Ecosyst. Heal. Manag.* **8** 251–7
[4] Sharma E, Molden D, Rahman A, Khatiwada Y R, Zhang L, Singh S P, Yao T and Wester P 2019 Introduction to the Hindu Kush Himalaya Assessment *The Hindu Kush Himalaya Assessment: Mountains, Climate Change, Sustainability and People* ed P Wester, A Mishra, A Mukherji and A B Shrestha (Cham: Springer International Publishing) pp 1–16
[5] Scott C A, Zhang F, Mukherji A, Immerzeel W, Mustafa D and Bharati L 2019 Water in the Hindu Kush Himalaya *The Hindu Kush Himalaya Assessment: Mountains, Climate Change, Sustainability and People* ed P Wester, A Mishra, A Mukherji and A B Shrestha (Cham: Springer International Publishing) pp 257–99
[6] ANDRITZ Solutions against hydro-abrasive erosion, Optimized Design and SXH coating
[7] Krella A 2020 Resistance of PVD coatings to erosive and wear processes: A review *Coatings* **10**
[8] Eltvik Mette 2013 *Sediment erosion in Francis turbines* (Norwegian University of Science and Technology)
[9] Gjøsæter K 2011 *Hydraulic Design of Francis Turbine Exposed to Sediment Erosion* (Norwegian University of Science and Technology)
[10] GE Hydro 2019 GE Renewable Energy
[11] Panta S, Lamsal M, Thapa B and Thapa B S 2014 Prediction of Turbine Needed For Future Hydropower Projects in Nepal *Hydro Nepal J. Water, Energy Environ.* **14** 23–6
[12] Thapa B, Shrestha R, Dhakal P and Thapa B S 2005 Problems of Nepalese hydropower projects due to suspended sediments *Aquat. Ecosyst. Heal. Manag.* **8** 251–7
[13] Gautam S, Neopane H P, Acharya N, Chitrakar S, Thapa B S and Zhu B 2020 Sediment erosion in low specific speed francis turbines: A case study on effects and causes *Wear* **442–443** 203152
[14] Tengs E, Storli P T and Holst M 2018 Optimization procedure for variable speed turbine design *Eng. Appl. Comput. Fluid Mech.* **12** 652–61
[15] Iliev I, Trivedi C and Dahlhaug O G 2019 Variable-speed operation of Francis turbines : A

review of the perspectives and challenges *Renew. Sustain. Energy Rev.* **103** 109–21
[16] Claude J-M 2017 Performances achieved to the Grid by a Full Power Converter Used in a Variable Speed Pumped Storage Plant *J. Phys. Conf. Ser.* **813**
[17] Hell J 2017 High Flexible Hydropower Generation concepts for future grids *J. Phys. Conf. Ser.* **813**
[18] Schafer D and Simond J J 1998 Adjustable speed asynchronous machine in hydro power plants and its advantages for the electric grid stability *Cigre*
[19] Ghimire A, Dahal D, Kayastha A, Chitrakar S, Thapa B S and Neopane H P 2020 Design of Francis turbine for micro hydropower applications *J. Phys. Conf. Ser.* **1608**
[20] Finne I 1960 Erosion of surfaces by Solid Particles *Wear* **3** 87–103
[21] Chitrakar S 2014 FSI Analysis of Francis Turbines Exposed to Sediment FSI Analysis of Francis Turbines Exposed to Sediment Erosion Sailesh Chitrakar
[22] Rakibuzzaman M, Kim H H, Kim K, Suh S H and Kim K Y 2019 Numerical study of sediment erosion analysis in Francis turbine *Sustain.* **11**
[23] ANSYS Inc. 2009 *ANSYS CFX-Solver Theory Guide* vol 15317
[24] Cavazzuti M 2013 *Optimization Methods: From Theory to Design* vol 53